Fiber Bragg Gratings for Strain and Temperature Measurements in a Smart Tire

G. Breglio, F. Fienga, A. Irace, M. Russo, S. Strano, M. Terzo

***Abstract*— In this paper, preliminary experimental results on strain and temperature distribution of the internal surface of a commercial tire coming from a Fiber Optical sensing system are presented. The measurement setup is based on Fiber Bragg Grating sensors (FBG) bonded in the internal surface of the tire in order to provide strain and temperature distributions during tire operation. Capabilities of the proposed method in terms of tire strain monitoring have been experimentally verified for several static vertical loads. The results have shown a clear correlation between strain, contact patch extension and vertical loads. Further tests have been executed for validating the optical sensing system in the case of thermal load application. The temperature measurement obtained by the FBG system confirmed a good accordance with the expected thermo-dynamic tire behavior.**

Index Terms*— Smart tires; strain monitoring; Fiber bragg gratings; tire temperature measurement.

I. Introduction

Tire road interaction strongly affects the vehicle dynamic behaviour because it represents the source of the input forces to the vehicle. As consequence, advances in this field are oriented to maximize the longitudinal and lateral forces between tire and road but, at the same time, to consider the tire through a systemic approach. So, the tire can be seen, from a mechanical point of view, the "actuator" of the vehicle but, at the same time, it can be seen also as a functional device for monitoring the interaction mechanism.

Research and technological advances in tire development are focused on the increasing of the vehicle safety, improving vehicle stability and control. Nowadays the vehicle safety relies more on active control systems that employ information about vehicle dynamics to improve the safety by detecting and minimizing skids [1].

G. Breglio is with the *Department of Electrical Engineering and Information Technologies, University of Naples Federico II*, 80125 ITALY (e-mail: breglio@unina.it).

F. Fienga is with the *Department of Electrical Engineering and Information Technologies, University of Naples Federico II*, 80125 ITALY (e-mail: francesco.fienga@unina.it).

A. Irace is with the *Department of Electrical Engineering and Information Technologies, University of Naples Federico II*, 80125 ITALY (e-mail: a.irace@unina.it).

M. Russo is with the *Department of Electrical Engineering and Information Technologies, University of Naples Federico II*, 80125 ITALY (e-mail: michele.russo@unina.it).

S. Strano is with the *Department of Industrial Engineering, University of Naples Federico II*, 80125 ITALY (corresponding author, phone: +390817683277; e-mail: salvatore.strano@unina.it).

M. Terzo is with the *Department of Industrial Engineering, University of Naples Federico II*, 80125 ITALY (e-mail: mario.terzo@unina.it).

Systems, such as Traction Control, Electronic Stability Program, etc., rely on the indirect estimation of vehicle dynamics variables, such as forces and tire road friction, using on board sensors. The instrumentation of the tire allows to make direct measurements with the fundamental advantage of obtaining information with higher accuracy. The consequence is that the so called "smart tire", that is the tire equipped with a sensor system for monitoring, for example, the tire strain, air pressure, acceleration or temperature is being researched extensively to improve the fuel efficiency, safety, and reliability of the vehicle [2 – 6].

The methods that involve the instrumentation of the tire are several: a tire equipped with a surface acoustic wave sensor has been developed in [7] to measure deformation, MEMS and optical fiber sensors have been employed in [8] and [9], respectively. Optical sensor technology has shown its advantages in terms of resolution, accuracy, power supply and data transmission [10].

Taking into account that the frictional mechanism is deeply linked to the mechanical properties and temperature of the materials, the present paper focuses on the direct measurement of the tire strain and rubber temperature with the aim to acquire direct information concerning the tire-road interaction and to realize an estimation of the friction conditions. The measurement setup is based on Fiber Bragg Grating (FBG) sensors bonded to the internal surface of the tire. Five sensors have been placed along the circumferential direction and four have been placed transversely. Vertical static tests and thermal tests have been executed in order to validate the functionalities of the proposed tire sensing system.

The paper is organized as follows. Section 2 presents the intelligent tire prototype system. In Section 3, the signals acquired during the experimental test campaign are presented. Section 4 draws some conclusions and presents some perspectives of the work.

II. Intelligent Tire Prototype System

A. Introduction and FBG

The aim of the experimental tests has been the measurement of temperature, and strain in several points inside a tire inner liner. Strain has been determined as a function of the vertical load and the inflation pressure. The measurements have been made using FBGs. An FBG is a distributed Bragg grating realized by periodically varying the core's refractive index in a short segment (10 mm) of a SM optical fiber, who reflects very narrowband of wavelengths of light and

ISBN: 978-988-14048-3-1
ISSN: 2078-0958 (Print); ISSN: 2078-0966 (Online)

transmits all others as depicted in (Fig. 1). A FBG can therefore be used as an inline optical filter to block certain wavelengths, or as a wavelength-specific reflector.

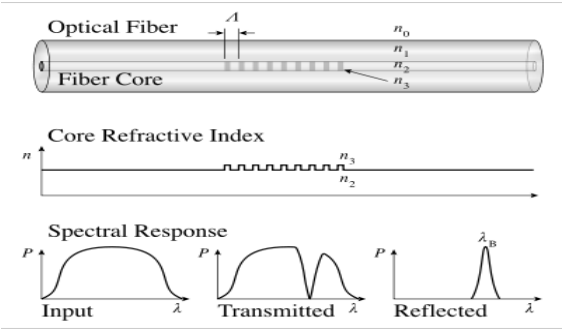

Fig. 1. Fiber Bragg Grating, refractive index profile and spectral response.

Light propagates through the grating with negligible attenuation or signal variation. Only those wavelengths that satisfy the Bragg condition are affected and strongly back-reflected. The ability to accurately preset and maintain the grating wavelength is a fundamental feature and advantage of fiber Bragg gratings. The central wavelength λ_B of the reflected component satisfies the Bragg relation:

$$\lambda_B = 2n_{eff}\Lambda \tag{1}$$

where n_{eff} is the effective index of refraction and Λ the period of the index of refraction variation of the FBG. Due to the temperature and strain dependence of the parameters n_{eff} and Λ, the wavelength of the reflected component will also change as function of temperature and/or strain. This dependency is well known and allows to determine the temperature or strain from the reflected FBG wavelength. Variations of physical properties of the grating sensor modify the reflected wavelength λ_B. In particular, strain on the fiber alters Λ and n through stress optic effect. Temperature variations modify n_{eff} via the thermos-optic effect and Λ is influenced by thermal expansion variations.

The instantaneous wavelength λ_i of the i-th FBG sensor is related to the local strain ε_i by the following formula:

$$\varepsilon_i = K_\varepsilon \frac{\lambda_i - \lambda_{0i}}{\lambda_{0i}} - \alpha\Delta T \tag{2}$$

where ΔT is the local temperature variation, α is the coefficient of thermal sensitivity, K_ε is the constant of proportionality and λ_{0i} is the reference wavelength for the i-th FBG sensor without any variation (both thermal and mechanical). In cases of temperature variations, two FBG sensors are required: one for the strain, which is mechanically bonded to the structure, and the other FBG, close to the first one, which is not bonded and consequently it is able to measure only temperature variations, which is used to depurate from the first one the wavelength shift due to the amount of the thermal apparent strain (as described in Eq. 2). As for instance, typical FBG sensor sensitivity to strain and temperature, at central wavelength around 1550um, are: wavelength variations due to mechanical strain about 1 pm/με and 10 pm/C°, respectively. Being wavelength encoded, FBG sensors allow distributed sensing over significant areas by multiplexing a large number of sensors on a single optical fiber and have compact size; moreover optical signals are intrinsically immune to electromagnetic interference. Due to all these advantages, they have been widely used in many applications for the structural health monitoring [10].

B. FBG-based intelligent tire

FBG sensors have been utilized to measure the local deformation and temperature of the tire carcass. The tire used for the actual setup has the size 245/40/R18. Fig. 2 shows the reference systems adopted for the pneumatic tire and the area in the inner surface where the FBGs have been bonded.

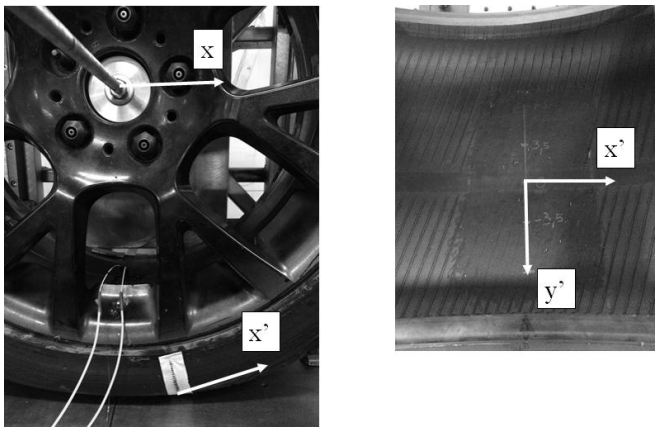

Fig. 2. Reference systems.

In this preliminary study, the tire has been deformed only statically and vertically for different tire-force relative direction. A practical implementation of the proposed intelligent tire is under development and an optical rotary joint or a wireless FBG interrogator should be necessary for dynamic tests in rolling conditions. An FBG interrogator, based on the use of tunable laser, has been adopted for measuring the frequency of the light reflected by FBG sensors from the various positions along the fiber where they are inserted. In particular, nine FBGs have been used for deformations; one has been used for temperature (Fig. 3). The connection between the fiber inside the tire and the interrogator has been executed through a hole in the tire rim, applying a sealant (see Fig. 2). The FBG sensors for strain measurement are schematized with gray rectangles in Fig. 3, while the FBG sensor for temperature measurement is depicted with a black rectangle. In particular, five deformation sensors have been placed in the circumferential direction (axis x') and four deformation sensors have been placed transversely (axis y').

ISBN: 978-988-14048-3-1
ISSN: 2078-0958 (Print); ISSN: 2078-0966 (Online)

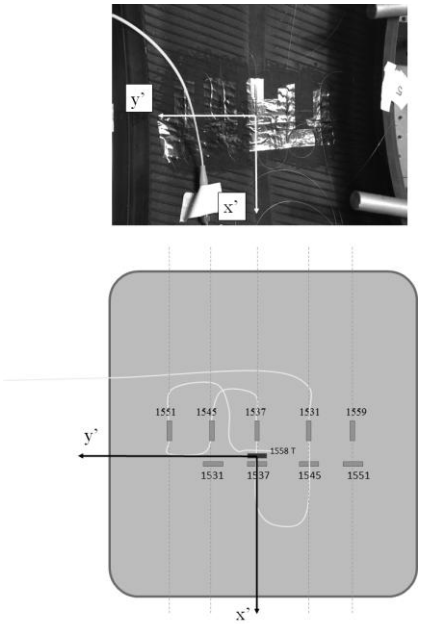

Fig. 3. Positions of the FBGs inside the tire. Numbers in the schetch refers to the cetral wavelengt of the single FBG.

The reference wavelength and the position of the i-th FBG sensor are indicated in Fig. 3. Table I shows the nomenclature adopted for the executed measurements.

TABLE I. NOMENCLAUTRE OF MEASUREMENTS

Measurements				
Type	***Symbol***	***λ_{0i}***	***x' (mm)***	***y' (mm)***
Lateral Deformation	ε_{y1}	1531	+22	+35
Lateral Deformation	ε_{y2}	1537	+22	0
Lateral Deformation	ε_{y3}	1545	+22	-35
Lateral Deformation	ε_{y4}	1551	+22	-75
Circonferential Deformation	ε_{x1}	1551	-3	+75
Circonferential Deformation	ε_{x2}	1545	-3	+35
Circonferential Deformation	ε_{x3}	1537	-3	0
Circonferential Deformation	ε_{x4}	1531	-3	-35
Circonferential Deformation	ε_{x5}	1559	-3	-75
Temperature	T	1531	0	0

III. EXPERIMENTAL RESULTS

A. Vertical load

Experimental tests have been developed with a specific test rig that has allowed to apply a vertical load to the tire by measuring the rim vertical displacement and the force. Fig. 4 shows the tire, the load cell for the vertical force measurement and the displacement sensor.

Fig. 4. Test rig.

Experiments have been executed with a tire inflation pressure equal to 2.3 bar. During the testing procedure, The vertical displacement for each load has been measured during the testing procedure.

Fig. 5 shows the definition of the rotation angle θ which has been used to specify the angular positions of the FBGs with reference to a vertical axis passing through the rim center. More specifically, the white marker in Fig. 5 identifies externally the center of the reference system shown in Fig. 3.

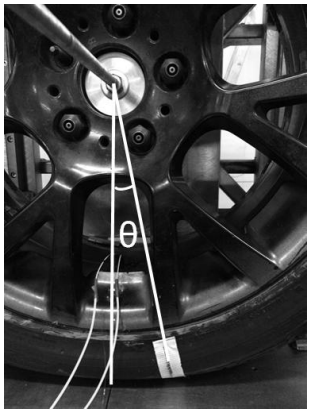

Fig. 5. Definition of the rotation angle θ.

Several static tests have been conducted varying the rotational angle θ in order to reconstruct the behavior of the strain measurements outside and inside the contact patch.

Fig. 6 and Fig. 7 show the circumferential strains ε_{x4} and ε_{x5} for three values of the vertical load: 1000 N, 1500 N, 2500 N.

ISBN: 978-988-14048-3-1
ISSN: 2078-0958 (Print); ISSN: 2078-0966 (Online)

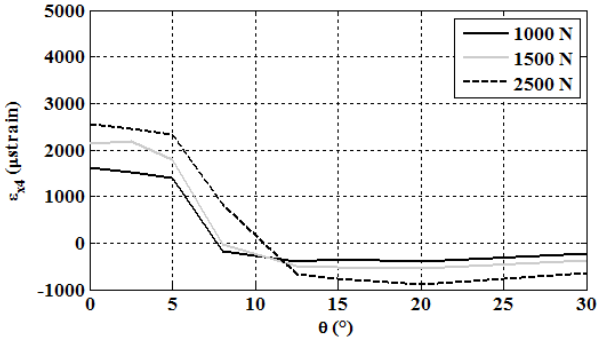

Fig. 6. Circumferential strain ε_{x4}.

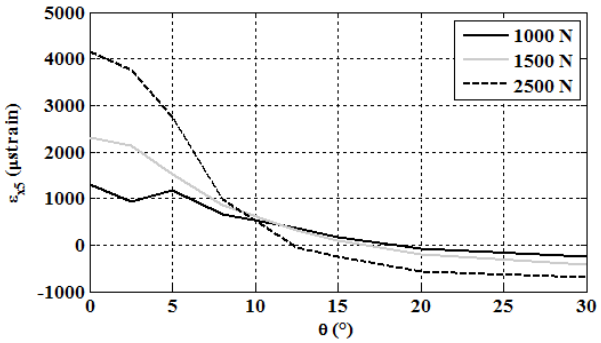

Fig. 7. Circumferential strain ε_{x5}.

The strain distributions of Figs. 6 and 7 clearly show that the maximum strain value for θ = 0° increases by increasing the vertical load, for both the circumferential strain sensors. These results can be useful in order to estimate the vertical load from the maximum value of the strain in the middle of the contact patch. Furthermore, using the relationship between the applied vertical load and the vertical displacement of the rim, the rolling radius can be estimated.

Compressive strains on the periphery of the contact patch are due to the carcass bending [11]. Therefore, the inner surface is under compression before entering the contact patch and after leaving the contact patch, and is stretched within the contact patch.

Fig. 8 and Fig. 9 show the lateral strains ε_{y2} and ε_{y3} for three values of the vertical load: 1000 N, 1500 N, 2500 N.

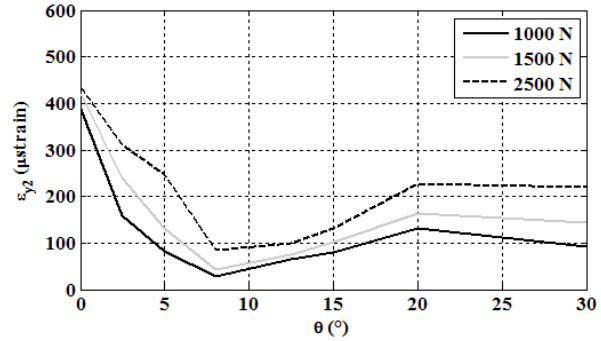

Fig. 8. Lateral strain ε_{y2}.

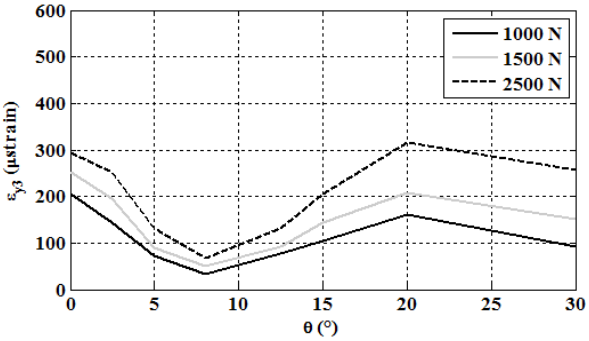

Fig. 9. Lateral strain ε_{y3}.

The lateral strains have their maximum values lower than those circumferential ones. The strain distributions show tensile stresses for all the values of the rotational angle. In the prossimity of the contact patch, lateral stains have a decreasing trend until reaching a minimum value, and then incresing up to the center of the contact patch.

An estimation of the contact length could be obtained by numerically differentiating the cricoferential strains with respect to the rotational angle [11]. Fig. 10 shows the behavior of the numerical differentation of circunferential strain ε_{x5} with respect to the rotation angle θ, for two vertical loads: 1000 N and 2500 N.

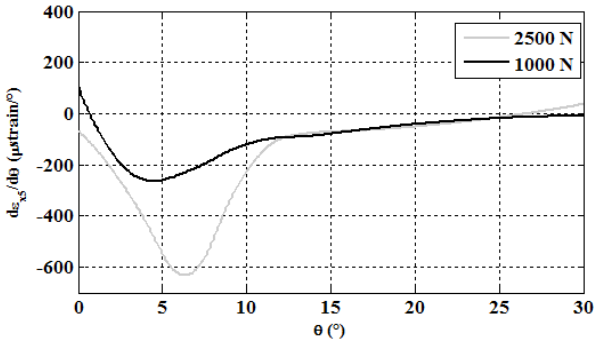

Fig. 10. Numerical differentation of circunferential strain ε_{x5} with respect to the rotation angle θ.

The angular extension of the contact patch is related to the value of the angle for which the derivative is minimum [11]. Consequently, the abscissa value at the minimum of the two graphs of Fig. 10 refers to the extension of the contact patch for the two vertical loads. Therefore, it is possible to note that the contact length increases by increasing the vertical load.

B. Temperature measurements

Thermal tests have been conducted heating the tire with a hot fan and by measuring the external temperature with a IR thermal camera and the temperature of the inner liner with the FBG sensor in contact with the rubber, where a thermally conductive paste has been applied (Fig. 11) to assure the heat transmission between the rubber and the fiber.

ISBN: 978-988-14048-3-1
ISSN: 2078-0958 (Print); ISSN: 2078-0966 (Online)

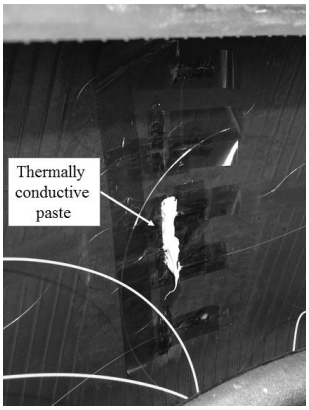

Fig. 11. Detail fo the thermally conductive paste used between the tire inner surface and the FBG.

Fig. 12 shows a camera frame acquired during the heating phase. The image presented in Fig. 12 clearly shows the external area of the tire invested by the hot air flow.

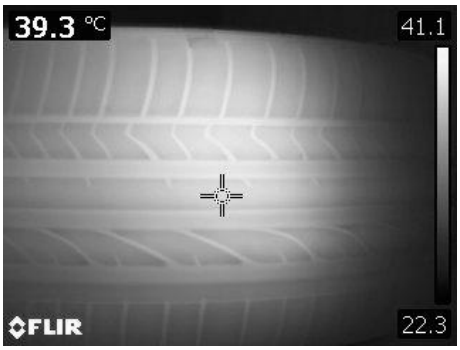

Fig. 12. Camera frame during the heating phase.

In Fig. 13, the trends of the outer and the inner temperature are reported. In particular, the test has been carried out by heating the tire up to 74 °C. Successively, the heat source has been interrupted.

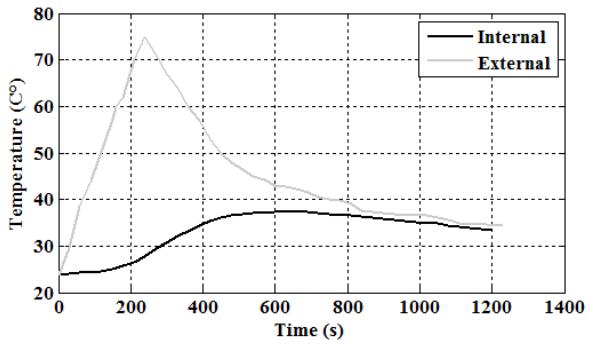

Fig. 13. External and internal temperature dynamic measured with the thermal camera and the FBG, respectively.

In Fig. 13, it is possible to note that towards the end of the test the outer and the inner temperature follow the same trend, in line with the expected thermal cooling process.

IV. Conclusions

An extensive experimental activity has been performed in order to equip a tire with FBG optical sensors to measure both temperatures and deformations of the tire inner surface. Vertical static tests have been developed to correlate the circumferential and the lateral deformation to the applied vertical load and contact patch. Similarly, thermal tests have allowed to analyze the thermal behavior of the tire inner surface. The optical sensors have provided measurements consistent with the expected physical behavior of the tire. The results could allow to validate various types of tire models; i.e. finite element tire models and thermo-dynamic tire models. The developed sensory system equipped with an optical rotary joint or a wireless system will allow to test the proposed smart tire in actual rolling condition.

Acknowledgment

The research activity is a result of partnership between University of Naples Federico II and OptoSmart s.r.l.

References

[1] R. Russo, S. Strano, M. Terzo, “Enhancement of vehicle dynamics via an innovative magnetorheological fluid limited slip differential,” Mechanical Systems and Signal Processing, vol. 70 – 71, pp. 1193 – 1208, 2016.

[2] M. Sergio, N. Manaresi, M. Tartagni, R. Canegallo and R. Guerrieri, “On a road tire deformation measurement system using a capacitive-resistive sensor,” Smart Mater. Struct., vol. 15, no. 6, pp. 1700–1706, 2006.

[3] G. Schimetta, F. Dollinger and R. Weigel, “A wireless pressure-measurement system using a SAW hybrid sensor,” Proc. 2000 IEEE Ultrasonic Symp. pp 445–448, 2000.

[4] X. Zhang, F. Wang, Z. Wang, W. Li and D. He, “Intelligent tires based on wireless passive surface acoustic wave sensors,” Proc. 7th Int. IEEE Conf. Intelligent Transportation Systems, 2004, pp 960–9644.

[5] J. D. Cullen, N. Arvanitis, J. Lucas and A. I. Al-Shamma’a, “In-field trials of a tire pressure monitoring system based on segmented capacitance rings,” Measurement, vol. 32, pp 181–192, 2002.

[6] C. Halfmann, M. Ayoubi and H. Holzmann, “Supervision of vehicles’ tire pressures by measurement of body accelerations,” Control Eng. Pract., vol. 5, no. 8, pp. 1151–1159, 1997.

[7] A. Pohl, R. Steindl and L. Reindl, “The ‘intelligent tire’ utilizing passive saw sensors—measurement of tire fiction,” IEEE Trans. Instrum. Meas., vol. 48, pp. 1041–1046, 1999.

[8] L. Cao, T. S. Kim, S. C. Mantell and D. L. Polla, “Simulation and fabrication of piezoresistive membrane type MEMS strain sensor,” Sens. Actuators, vol. 80, pp. 273–279, 2000.

[9] N. Roveri, G. Pepe, A. Carcaterra, “OPTYRE – A new technology for tire monitoring: Evidence of contact patch phenomena,” Mechanical Systems and Signal Processing, vol. 66–67, pp. 793-810, 2016.

[10] F. Fienga, N. Beni, G. Breglio, S. Buontempo, M. Consales, A. Cusano, A. Gaddi, A. Irace, M. Giordano, S. Szillasi, “Fibre optic sensors structural health monitoring of the central beam pipe in the CMS experiment at the CERN laboratories,” 8th European Workshop on Structural Health Monitoring, EWSHM 2016, vol. 2, pp. 1018-1025, 2016.

[11] M. Ryosuke, H. Naoki, T. Akira, M. Yoshihiro, “Analysis of Applied Load Estimation Using Strain for Intelligent Tires,” Journal of Solid Mechanics and Materials Engineering, vol. 4, no. 10, pp. 1496–1510, 2010.

ISBN: 978-988-14048-3-1
ISSN: 2078-0958 (Print); ISSN: 2078-0966 (Online)